This article was downloaded by: [University of Haifa Library]
On: 10 September 2013, At: 00:18
Publisher: Taylor & Francis
Informa Ltd Registered in England and Wales Registered Number: 1072954 Registered office: Mortimer House, 37-41 Mortimer Street, London W1T 3JH, UK

Liquid Crystals
Publication details, including instructions for authors and subscription information:
http://www.tandfonline.com/loi/tlct20

Cholesterol-based unsymmetrical Schiff's base dimer terminated with 4-alkoxy-5-phenylthiophene unit: synthesis and characterisation

K.C. Majumdar [a], Tapas Ghosh [a], Santanu Chakravorty [a], Nilashis Pal [a], D.S. Shankar Rao [b] & S. Krishna Prasad [b]

[a] Department of Chemistry, University of Kalyani, West Bengal, India

[b] Centre for Liquid Crystal Research (CLCR), Jalahalli, Bangalore, India

Published online: 10 Dec 2010.

To cite this article: K.C. Majumdar , Tapas Ghosh , Santanu Chakravorty , Nilashis Pal , D.S. Shankar Rao & S. Krishna Prasad (2010) Cholesterol-based unsymmetrical Schiff's base dimer terminated with 4-alkoxy-5-phenylthiophene unit: synthesis and characterisation, Liquid Crystals, 37:12, 1539-1547, DOI: 10.1080/02678292.2010.526721

To link to this article: http://dx.doi.org/10.1080/02678292.2010.526721

PLEASE SCROLL DOWN FOR ARTICLE

Taylor & Francis makes every effort to ensure the accuracy of all the information (the "Content") contained in the publications on our platform. However, Taylor & Francis, our agents, and our licensors make no representations or warranties whatsoever as to the accuracy, completeness, or suitability for any purpose of the Content. Any opinions and views expressed in this publication are the opinions and views of the authors, and are not the views of or endorsed by Taylor & Francis. The accuracy of the Content should not be relied upon and should be independently verified with primary sources of information. Taylor and Francis shall not be liable for any losses, actions, claims, proceedings, demands, costs, expenses, damages, and other liabilities whatsoever or howsoever caused arising directly or indirectly in connection with, in relation to or arising out of the use of the Content.

This article may be used for research, teaching, and private study purposes. Any substantial or systematic reproduction, redistribution, reselling, loan, sub-licensing, systematic supply, or distribution in any form to anyone is expressly forbidden. Terms & Conditions of access and use can be found at http://www.tandfonline.com/page/terms-and-conditions

Liquid Crystals,
Vol. 37, No. 12, December 2010, 1539–1547

Taylor & Francis
Taylor & Francis Group

Cholesterol-based unsymmetrical Schiff's base dimer terminated with 4-alkoxy-5-phenylthiophene unit: synthesis and characterisation

K.C. Majumdar[a]*, Tapas Ghosh[a], Santanu Chakravorty[a], Nilashis Pal[a], D.S. Shankar Rao[b] and S. Krishna Prasad[b]

[a]*Department of Chemistry, University of Kalyani, West Bengal, India;* [b]*Centre for Liquid Crystal Research (CLCR), Jalahalli, Bangalore, India*

(*Received 24 August 2010; final version received 21 September 2010*)

A series of unsymmetrical cholesterol based dimers have been synthesised and characterised. All the dimers possess a cholesterol unit connected with a 4-alkoxy-5-phenylthiophene unit through Schiff's base linkage. The length of the terminal alkyl and the alkyl spacer has been varied. All the dimers exhibit mesomorphism. Four dimers possess only the cholesteric (chiral nematic, N*) phase. One of the dimers showed smectic A (SmA) and N* phases whereas the other dimer displayed SmA, smectic chiral C (SmC*), N* and twist grain boundary (TGB) phases.

Keywords: thiophene; dimers; SmA; SmC*; N*; TGB phase; HRXRD

Downloaded by [University of Haifa Library] at 00:18 10 September 2013

1. Introduction

Heterocycles are used mostly as core units in thermotropic liquid crystals because of their ability to impart lateral and/or longitudinal dipole combined with changes in molecular shapes. These materials hold great potential for use in spatial light modulation [1], all optical signal processing, optical information storage [2], organic thin film transistors [3, 4], fast switching ferroelectric materials [5], fluorescent probes for the detection and analysis of biomolecules [6], etc. Among the heterocycles, thiophene in particular has emerged as a core unit for liquid crystalline material over the last few years. Materials that contain a thiophene core have significant lateral dipole moments, which contribute to their physical parameters such as increased dielectric anisotropy and dielectric biaxiality. The latter property allows for AC field stabilisation, a feature that is currently essential for ferroelectric device operation [7, 8].

Symmetrical and unsymmetrical dimers, in which mesogenic segments connected through a flexible paraffinic central spacer, have attracted a great deal of attention over the years [9–27]. The main reason behind this is that for polymeric liquid crystals symmetrical dimers are regarded as model compounds while the unsymmetrical dimers exhibit a wide range of smectic phases [28–30]. Moreover, chiral unsymmetrical dimers, in particular compounds possessing a cholesteryl ester unit joined to different aromatic mesogens through an alkyne spacer, show interesting thermal behaviour [31–41]. In the cholesterol-based unsymmetrical dimers the cholesterol unit is connected to a variety of aromatic/aromatic-alicyclic cores, namely Schiff's base, tolane, azobenzene, biphenyl, chalcone, cyclohexane, phenyl benzoate, salicylaldimine, stilbene, etc. In this context, we have undertaken a study to synthesise a series of unsymmetrical dimers in which the cholesterol unit is connected with the 4-alkoxy substituted phenyl thiophene unit via a flexible Schiff's base linkage and have investigated their liquid crystalline behaviour.

2. Results and discussion

A series of unsymmetrical dimers for this study were prepared in several steps starting from cholesterol as depicted in Scheme 1. Reaction between cholesterol and 6-bromohexanoyl chloride in tetrahydrofuran (THF) at room temperature gave the corresponding ester derivatives **3.** The ester derivatives were then subjected to alkylation with *p*-hydroxybenzaldehyde in refluxing acetone in the presence of anhydrous K_2CO_3 to give the corresponding aldehydes **4.** On the other hand, 5-(4′-alkoxy phenyl)-2-aminothiophenes **9a–c** were synthesised in six steps starting from 2-bromo thiophene **4**. The nitration of 2-bromothiophene was carried out by using nitric acid–acetic anhydride mixtures to give the corresponding nitro derivative **5**. The Suzuki cross coupling between 4-alkoxy boronic acid **7a–c** derivatives and 2-bromo-5-nitrothiophene gave the corresponding 5-(4′-alkoxyphenyl)-2-nitrothiphene derivatives **8a–c**, which on subsequent hydrogenation yielded the corresponding amine derivatives **9a–c**. The condensation reaction

*Corresponding author. Email: kcm_ku@yahoo.co.in

ISSN 0267-8292 print/ISSN 1366-5855 online
© 2010 Taylor & Francis
DOI: 10.1080/02678292.2010.526721
http://www.informaworld.com

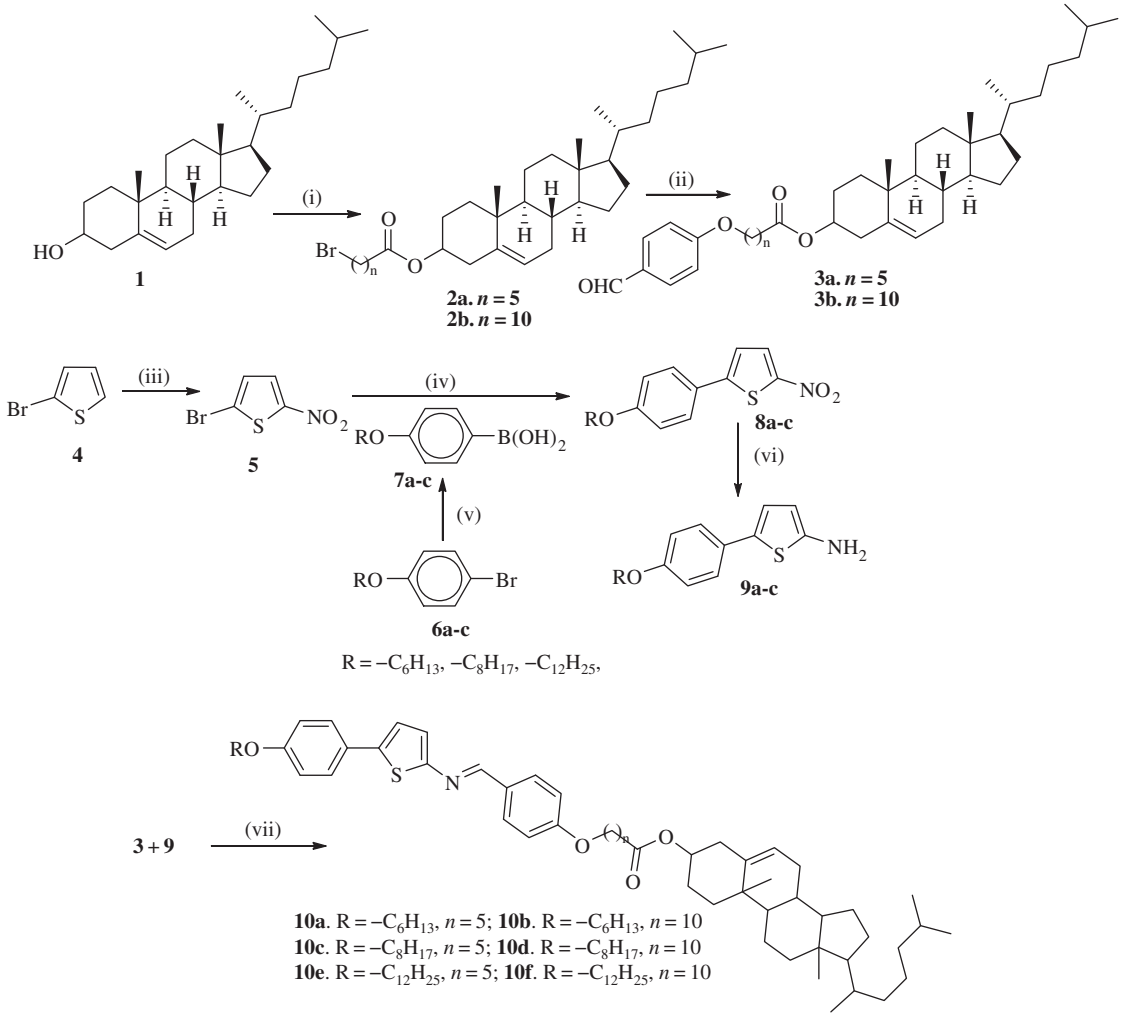

Scheme 1. Reagents and conditions: (i) bromoalkanoyl chloride, tetrahydrofuran (THF), pyridine, room temperature (rt), (ii) p-hydroxy benzaldehyde, acetone, K_2CO_3, reflux, (iii) HNO_3, acetic anhydride, icebath, (iv) $Pd(PPh_3)4$, 2.0 M aq. Na_2CO_3, (v) n-BuLi, $B(OMe)_3$, THF, −78°C rt, (vi) H_2, Pd/C, rt, (vii) dry alcohol, acetic acid (cat), reflux.

between aldehydes and amines gave a series of unsymmetrical Schiff's base derivatives **10a–f**.

The thermotropic properties were studied by polarised optical microscopy (POM) and differential scanning calorimetry (DSC) and the results are summarised in Table 1. Compounds **10b**, **10d** and **10f** having long alkyl chain spacers ($n = 10$) exhibit only one mesophase as suggested by calorimetry. Compounds **10d** and **10f** show two peaks both in the heating as well as in the cooling cycles of the DSC experiments (both the heating and cooling rates are 5°/min). However, compound **10b** exhibits three peaks in the heating cycles but only one peak in the cooling cycle in the DSC thermogram. The peak at 98.6°C in the heating cycle is due to a solid–solid transition.

Compound **10f** when placed in a thin cell of thickness $d = 5 \pm 0.2$ μm and cooled slowly from its isotropic temperature exhibits the characteristic oily-streak texture of the cholesteric (chiral nematic, N*) phase (Figure 1). Compound **10f** also exhibits the fan-like textures of the cholesteric phase when placed in between the glass plates. Compounds **10b** and **10d** exhibit similar types of textures. Compound **10b**, which does not show any peak in the cooling cycle in the DSC thermogram, solidifies on cooling at about 75°C.

Compounds **10a**, **10c** and **10e** having short alkyl chain spacers ($n = 5$) do not follow any of the usual trends (exhibition of only the N* phase) as exhibited by their long chain counterparts. Compound **10a** shows two peaks in the heating cycle but only one peak in the cooling cycle of the DSC experiment. Compounds **10c** and **10e** exhibit four peaks in the heating cycles and only three peaks in the cooling cycles of the DSC thermogram. Compound **10a** when sandwiched between two glass plates and cooled

Downloaded by [University of Haifa Library] at 00:18 10 September 2013

Table 1. Transition temperature (°C) and associated enthalpies (kJmol^{-1}) recorded "from the DSC experiment".

10a: Cr $\xrightarrow[109.0]{[18.2]}$ N* $\xrightarrow[224.2]{[1.0]}$ I $\xrightarrow[214.9]{[1.0]}$ N* $\xrightarrow[108.0]{[POM]}$ Cr

10b: Cr $\xrightarrow[98.6]{[3.9]}$ Cr_1 $\xrightarrow[111.3]{[13.4]}$ N* $\xrightarrow[168.3]{[0.8]}$ I $\xrightarrow[166.7]{[0.8]}$ N* $\xrightarrow[75.0]{[POM]}$ Cr

10c: Cr $\xrightarrow[66.8]{[68.0]}$ Cr_1 $\xrightarrow[109.7]{[7.9]}$ Cr_2 $\xrightarrow[134.6]{[6.0]}$ N* $\xrightarrow[215.3]{[1.8]}$ I $\xrightarrow[214.6]{[2.9]}$ N*

N* $\xrightarrow[179.0]{[...]}$ SmA - - - - - - - TGB

SmA $\xrightarrow[127.0]{[...]}$ SmC $\xrightarrow[68.3]{[0.3]}$ Cr_1 $\xrightarrow[61.4]{[0.4]}$ Cr

10d: Cr $\xrightarrow[83.6]{[18.1]}$ N* $\xrightarrow[169.2]{[1.0]}$ I $\xrightarrow[167.6]{[1.0]}$ N* $\xrightarrow[62.2]{[5.1]}$ Cr

10e: Cr $\xrightarrow[87.8]{[2.5]}$ Cr_1 $\xrightarrow[106.8]{[18.4]}$ SmA $\xrightarrow[209.4]{[3.7]}$ N* $\xrightarrow[226.3]{[0.02]}$ I $\xrightarrow[226.2]{[0.02]}$ N*

N* $\xrightarrow[207.1]{[3.6]}$ SmA $\xrightarrow[53.9]{[6.3]}$ Cr

10f : Cr $\xrightarrow[112.3]{[58.2]}$ N* $\xrightarrow[163.8]{[1.0]}$ I $\xrightarrow[162.6]{[1.1]}$ N* $\xrightarrow[72.0]{[31.0]}$ Cr

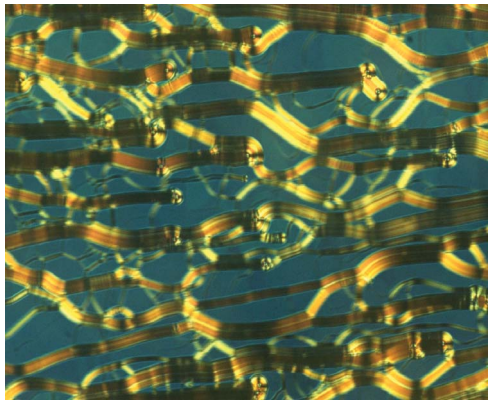

Figure 1. The texture of compound **10f** at 159°C (colour version online).

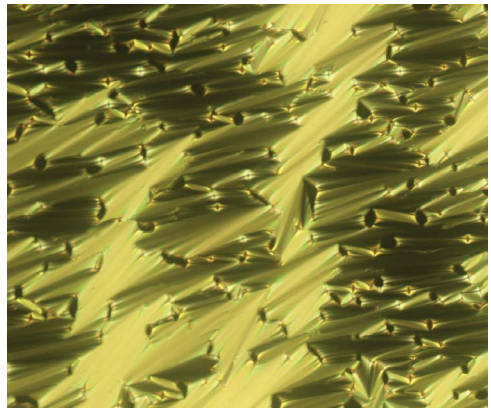

Figure 2. The texture of compound **10e** at 204°C (colour version online).

slowly from its isotropic temperature exhibits the characteristic texture of the cholesteric (N*) phase [42] and on further cooling solidifies at about 110°C. On cooling the isotropic phase of compound **10e**, elliptical shaped droplets appear, which coalesce to form fan like texture characteristic of cholesteric (N*) phase. On further cooling, the sample exhibits the homeotropic texture of the smectic A (SmA) phase. For compound **10e,** when placed in a thin cell with a cell gap of $d = 5 \pm 0.2$ μm with homogeneous planar boundary conditions, the textures of the cholesteric and smectic phases (Figure 2) were observed. In this arrangement, the long molecular axes are oriented in the plane of the substrate and the helix axis of the N* phase is perpendicular to the boundary glass plates.

Compound **10c** on cooling (when sandwiched in a glass plate from its isotropic temperature) exhibits first an N* phase, then on further cooling a phase change

Downloaded by [University of Haifa Library] at 00:18 10 September 2013

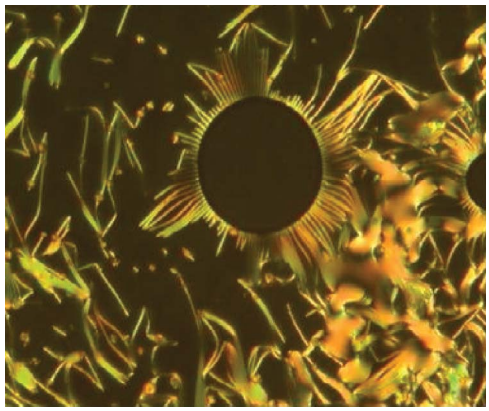

Figure 3. The Cholesteric–TGB–SmA transition of compound **10c** at 179°C (colour version online).

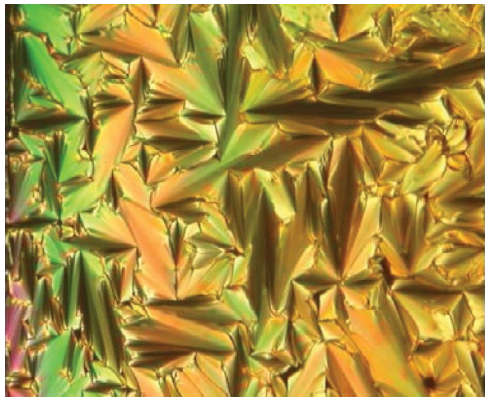

Figure 4. The texture of compound **10c** at 175°C (colour version online).

occurs with the appearance of a filament texture characteristic of a TGB phase [43] from the cholesteric region and then it finally shows a dark field of view in the SmA phase. When the sample was placed in a thin cell and cooled slowly the characteristic textures of the N*, TGB (Figure 3) and SmA (Figure 4) phases appear gradually from the isotropic melt. On further cooling a phase change occurs at around 127°C after which the typical schlieren texture of the chiral smectic C (SmC*) phase (Figure 5) appears and exists until solidification. However, we did not observe any phase transition corresponding to the N*→SmA and SmA→SmC* transitions in the DSC experiment even at a rate of 3°/min. The DSC thermograms of compounds **10b** and **10e** exhibit low clearing entropies. This may be interpreted in terms of the increased biaxiality of the cholesteryl-based group compared to a conventional biphenyl mesogenic unit [44–49].

To confirm the nature of the SmA and SmC* phases of compound **10c**, X-ray diffraction (XRD) experiments were performed using an image plate apparatus [50]. The diffraction patterns obtained in

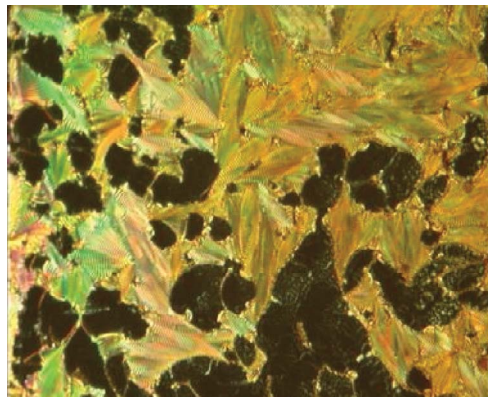

Figure 5. The texture of compound **10c** at 120°C (colour version online).

the two phases at 140°C and 120°C respectively are shown in Figure 6(a). Both the patterns exhibit a liquid-like peak at wide angles and a single sharp peak at low angles confirming the layer structure of the phases. The layer thickness value corresponding to the low angle reflection in the SmA phase is 51.0 Å and much lower (47.6 Å), as expected, in the SmC* phase. The all-*trans* molecular length of this dimer (**10c**), as obtained from the MM2 energy minimisation package of the CS Chem3D software, is 51.2 Å. This indicates that the layer spacing in the SmA phase is very close to that of the molecular length and thus the phase is a monolayer smectic. The energy minimised configuration (Figure 6(b)) displays that the molecule has essentially a rod-like shape. The X-ray spacing value obtained in the SmC* phase corresponds to a tilt angle

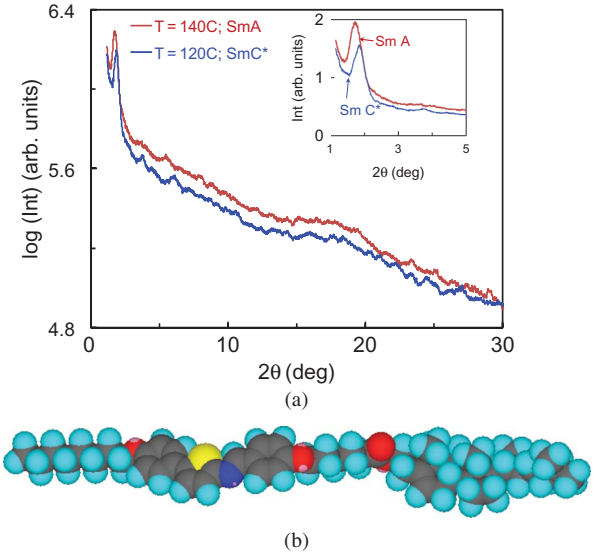

Figure 6. (a) XRD diagram of compound **10c** in the SmA and SmC phases. The inset shows the low angle reflections on an enlarged scale. (b) Energy minimised configuration of the molecule **10c** obtained using the MM2 package (colour version online).

Downloaded by [University of Haifa Library] at 00:18 10 September 2013

Downloaded by [University of Haifa Library] at 00:18 10 September 2013

of 20 degrees (assuming a rigid-rod tilt), a feature compatible with the second-order nature of the transition observed in the DSC experiments.

Kelly and co-workers reported in [51] the behaviour of light emitting liquid crystal trimers consisting of two dihydrocholesteryl groups and an extended aromatic core containing a thiophene ring. These trimers exhibited a N* phase and in addition a SmC* phase. Yeap *et al.* [52] synthesised and characterised a series of non-symmetric liquid crystal dimers, α-(4-benzylidenechloroaniline-4′-oxy)-ω-[4-(thiophene-2-carboxyl)benzylideneaniline-4′-oxy]alkanes incorporating a thiophene-based moiety in one of the two mesogenic units. The nematogenic properties of the dimers were studied wherein the flexible spacers made up of *N*-methylene units $(-CH_2-)_n$ ranging from $n = 5$ to $n = 12$. These dimers exhibited an enantiotropic nematic phase with high thermal stability. Seed *et al.* [53] synthesised a variety of thiophene containing materials for use in electro-optic devices and most of them exhibited a nematic phase. There are several examples of cholesterol-based liquid crystalline Schiff's base dimers but to the best of our knowledge these may be the first examples of cholesterol-based unsymmetrical dimers with an alkoxy substituted 5-phenylthiophene unit.

2.1 *Optical properties*

The ultraviolet-visible absorption and fluorescence spectra of the compounds **10a–f** in $CHCl_3$ solution are shown in Figures 7 and 8, respectively and Table 2. The absorption spectra of all the compounds **10a–f** were very similar in shape due to their structural similarity. The highest absorption peaks of all the compounds were found to be near 396 nm. The absorbance is a maximum in the case of compound **10b** and for compound **10d** the absorbance is a minimum. On the other hand, the fluorescence spectra of compounds **10c–f** are all triplet in nature. However, for compounds **10a,b** the curves are of singlet pattern and the maxima shifted to higher wavelength. The red shift in the case of **10a** and **10b** may be due to the perturbation of the excited singlet state in a stabilising manner. Structured emission bands for compounds **10c–f** are possibly due to the chain length effect.

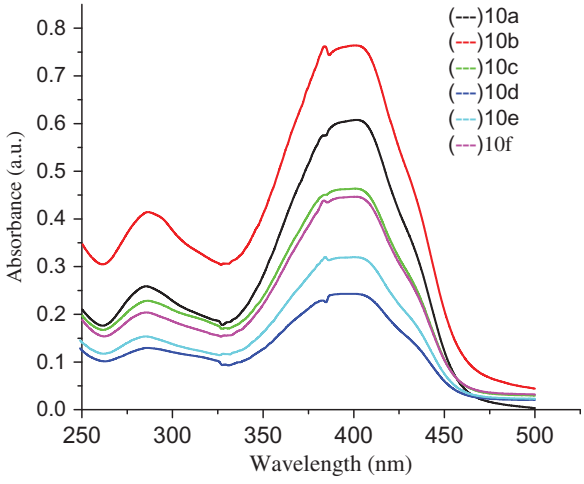

Figure 7. UV-visible spectra of compounds **10a–f** in $CHCl_3$ (colour version online).

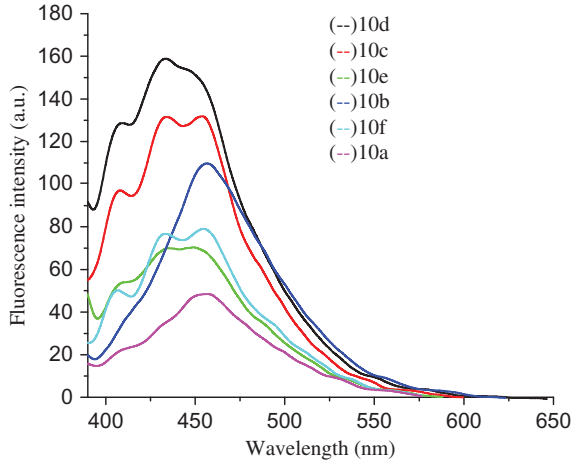

Figure 8. Fluorescence spectra of compounds **10a–f** in $CHCl_3$ at 380 nm (colour version online).

Table 2. UV and fluorescence peaks for compounds **10a–10f**.

Compounds	UV (nm)	Fluorescence (nm)
10a	285, 398	455
10b	286, 398	456
10c	286, 396	407, 433, 453
10d	285, 396	408, 433, 451
10e	284, 396	408, 434, 451
10f	285, 396	406, 433, 454

In conclusion, we have synthesised a series of unsymmetrical liquid crystalline dimers in which the cholesterol unit is connected with the alkoxy substituted 5-phenylthiophene unit via a Schiff's base linkage. We have varied the lengths of the terminal alkyl chain and the alkyl spacer. The dimers with long alkyl spacers ($n = 10$) exhibit only the N* phase, while some of the dimers with short alkyl spacers ($n = 5$) exhibit a variety of phase sequences.

3. Experimental details

All the chemicals were procured from either Sigma Aldrich Chemicals Pvt. Ltd. or Spectrochem, India. Silica gel (60–120 mesh) was used for the chromatographic separation. Silica gel G (E-Merck

Downloaded by [University of Haifa Library] at 00:18 10 September 2013

(India)) was used for thin layer chromatography (TLC). Petroleum ether refers to the fraction boiling between 60°C and 80°C. Infrared (IR) spectra were recorded on a Perkin-Elmer L 120-000A spectrometer (ν_{max} in cm^{-1}) on KBr discs. ^1H NMR (400 MHz, 500 MHz) spectra were recorded on a Bruker DPX-400, Bruker DPX-500 spectrometer in $CDCl_3$ (chemical shift in δ) with tetramethylsilane (TMS) as internal standard. The liquid crystalline properties were established by thermal microscopy (Nikon polarising microscope LV100POL attached to Instec hot and cold stage HCS302, with STC200 temperature controller configured for HCS302) and the phase transitions were confirmed (both heating and cooling rates were 5°/min) by differential scanning calorimetry (Perkin-Elmer DSC Pyris1 system). The high-resolution XRD was carried out at CLCR, Bangalore.

3.1 General procedure for the preparation of compounds 2 and 3

Compounds **2** and **3** were prepared according to the previously published procedure [12].

3.2 General procedure for the preparation of compounds 5–9

The nitration of 2-bromothiophene was carried out with HNO_3 in the presence of acetic anhydride in an ice bath. Compound **4** (3.1 g, 0.02 mol) was dissolved in acetic anhydride (6.25 ml) and stirred vigorously at −5° to 0°C. To this stirred solution, concentrated HNO_3 (4.0 ml) and acetic anhydride (6.25 ml) were added drop wise so that the temperature was kept below 0°C. After completion of the addition, the reaction mixture was kept in an ice bath and stirred for 30 min and then left in a refrigerator overnight. Then the reaction mixture was poured onto ice and the solid was filtered off. The solid was dissolved in ether and the organic phase was washed with water (3 × 20 ml) and dried (Na_2SO_4). The residue obtained after removing the solvent was subjected to column chromatography over silica gel using petroleum ether/ethyl acetate (49:1) as eluent to give the product **5**. On the other hand, boronic acid precursors **7a–c** were prepared from appropriate alkoxybromides via the halogen metal exchange reaction. Compound **6a** (2.0 g, 7.75 mmol) was dissolved in dry THF (20 ml), cooled to −78°C. To this solution n-butyl lithium (6.2 ml, 9.3 mmol) was added drop wise and stirred for an additional 30 min. Trimethyl borate (1.75 g, 17.05 mmol) was dissolved in dry THF and was added drop wise to the stirred solution. After completion of the addition, the solution was stirred for a further 2 h at −78°C and then stirred overnight at room temperature 20 ml. 10% HCl solution was then added to hydrolyse the borate esters and was stirred for 1 h. The resulting solution was extracted with ether (2 × 30 ml) and the organic phase was washed with water (3 × 15 ml) and dried (Na_2SO_4). The solvent was distilled off and the residual mass was subjected to column chromatography over silica gel using petroleum ether/ethyl acetate (4:1) as eluent to produce the product **7a.** The compounds **7b** and **7c** were prepared using the same procedure.

The boronic acid derivative **7a** was then used successfully in a subsequent palladium catalysed Suzuki cross coupling reaction with 2-bromo-5-nitrothiophene to give the corresponding nitro derivative **8a**. Compound **7a** (410 mg, 1.846 mmol) in EtOH (5 ml) was added to compound **5** (384 mg, 1.846 mmol) in benzene (10 ml). Then 2(M) aq. Na_2CO_3 (1.84 ml) solution was added to the reaction mixture followed by $Pd(PPh_3)_4$ (106 mg, 5 mol%), and the mixture was stirred at 110°C for 2 h. The reaction mixture was then extracted with $CHCl_3$ (2 × 20 ml) and the organic layer was washed with water (3 × 10 ml) and dried (Na_2SO_4). The solvent was distilled off and the residual mass was purified by column chromatography over silica gel using petroleum ether/ethyl acetate (19:1) as eluent to give the product **8a.** Compounds **8b** and **8c** were prepared accordingly.

The nitro derivative **8a** (400 mg, 1.42 mmol) was dissolved in 25 ml ethyl acetate, 15 mg of 10 mol% Pd/C was added to it followed by stirring under a hydrogen atmosphere for 12 h before being filtered through celite to remove the catalyst. The residual mass left after removing the solvent was then purified by column chromatography over silica gel using petroleum ether/ethyl acetate (19:1) as eluent to give the amine **9a.** Compounds **9b** and **9c** were prepared similarly.

Compound 8a: Yellow solid, yield 90%, melting point (m.p.) 68–70°C, IR (KBr) ν_{max}: 2918, 1603, 1540, 1329 cm^{-1}; ^1H-NMR ($CDCl_3$, 400 MHz): $\delta_H = 7.81$ (d, 1H, $J = 4.4$ Hz), 7.48 (d, 2H, $J = 8.8$ Hz), 7.05 (d, 1H, $J = 4.4$ Hz), 6.87 (d, 2H, $J = 8.8$ Hz), 3.92 (t, 2H, $J = 6.8$ Hz), 1.70 (quint., 2H, $J = 7.2$ Hz), 1.18–1.42 (m, 6H), 0.84 (t, 3H, $J = 6.8$ Hz). Anal. Calcd. for $C_{16}H_{19}NO_3S$: C, 62.93, H, 6.27, N, 4.59; found: C, 62.83, H, 6.29, N, 4.73.

Compound 8b: Yellow solid, yield 94%, m.p. 64–66°C, IR (KBr) ν_{max}: 2912, 1605, 1546, 1327 cm^{-1}; ^1H-NMR ($CDCl_3$, 400 MHz): $\delta_H = 7.86$ (d, 1H, $J = 4.4$ Hz), 7.52 (d, 2H, $J = 8.8$ Hz), 7.10 (d, 1H, $J = 4.4$ Hz), 6.89 (d, 2H, $J = 8.8$ Hz), 3.93 (t, 2H, $J = 6.4$ Hz), 1.77 (quint., 2H, $J = 6.8$ Hz), 1.20–1.41 (m, 10H), 0.85 (t,

Downloaded by [University of Haifa Library] at 00:18 10 September 2013

3H, J = 6.8 Hz). Anal. Calcd. for $C_{18}H_{23}NO_3S$: C, 64.84, H, 6.95, N, 4.20; found: C, 64.71, H, 6.79, N, 4.03.

Compound 8c: Yellow solid, yield 92%, m.p. 62–64°C, IR (KBr) ν_{max}: 2910, 1605, 1543, 1326 cm^{-1}; ^{1}H-NMR ($CDCl_3$, 400 MHz): δ_H = 7.88 (d, 1H, J = 4.4 Hz), 7.55 (d, 2H, J = 8.8 Hz), 7.12 (d, 1H, J = 4.4 Hz), 6.94 (d, 2H, J = 8.8 Hz), 3.95 (t, 2H, J = 6.4 Hz), 1.77 (quint., 2H, J = 6.4 Hz), 1.26–1.46 (m, 18H), 0.83 (t, 3H, J = 6.8 Hz). Anal. Calcd. for $C_{22}H_{31}NO_3S$: C, 67.83, H, 8.02, N, 3.60; found: C, 67.68, H, 8.13, N, 3.39.

Compound 9a: Brown solid, yield 94%, m.p. 82–84°C, IR (KBr) ν_{max}: 2923, 2853, 1605, 1573, 1392 cm^{-1}; ^{1}H-NMR ($CDCl_3$, 400 MHz): δ_H = 7.75 (d, 1H, J = 4.0 Hz), 7.43 (d, 2H, J = 8.4 Hz), 7.29 (d, 1H, J = 3.6 Hz), 6.83 (d, 2H, J = 8.4 Hz), 3.99 (t, 2H, J = 6.8 Hz), 1.77 (quint., 2H, J = 6.8 Hz), 1.25–1.46 (m, 6H), 0.88 (t, 3H, J = 6.8 Hz). Anal. Calcd. for $C_{16}H_{21}NOS$: C, 69.78, H, 7.69, N, 5.09; found: C, 69.68, H, 7.73, N, 5.26.

Compound 9b: Brown solid, yield 95%, m.p. 74−76°C, IR (KBr) ν_{max}: 2924, 2849, 1607, 1573, 1390 cm^{-1}; ^{1}H-NMR ($CDCl_3$, 400 MHz): δ_H = 7.76 (d, 1H, J = 4.0 Hz), 7.48 (d, 2H, J = 8.8 Hz), 7.28 (d, 1H, J = 4.0 Hz), 6.84 (d, 2H, J = 8.4 Hz), 3.99 (t, 2H, J = 6.8 Hz), 1.78 (quint., 2H, J = 6.8 Hz), 1.26–1.45 (m, 10H), 0.88 (t, 3H, J = 6.8 Hz). Anal. Calcd. for $C_{18}H_{25}NOS$: C, 71.24, H, 8.30, N, 4.62; found: C, 71.06, H, 8.13, N, 4.46.

Compound 9c: Deep brown solid, yield 92%, m.p. 70−72°C, IR (KBr) ν_{max}: 2921, 2850, 1605, 1571, 1392 cm^{-1}; ^{1}H-NMR ($CDCl_3$, 400 MHz): δ_H = 7.61 (d, 1H, J = 4.0 Hz), 7.50 (d, 2H, J = 8.4 Hz), 7.35 (d, 1H, J = 4.0 Hz), 6.84 (d, 2H, J = 8.8 Hz), 3.93 (t, 2H, J = 6.8 Hz), 1.77 (quint., 2H, J = 6.8 Hz), 1.27–1.46 (m, 18H), 0.87 (t, 3H, J = 6.8 Hz). Anal. Calcd. for $C_{22}H_{33}NOS$: C, 73.49, H, 9.25, N, 3.90; found: C, 73.33, H, 9.03, N, 4.04.

3.3 General procedure for the preparation of compounds 10a–f

A mixture of amine **9a** (100 mg, 0.36 mmol) and aldehyde **3a** (219.9 mg, 0.36 mmol) was refluxed in absolute ethanol (10 ml) in the presence of a catalytic amount of glacial acetic acid for 4 h. The Schiff's base **10a** (green solid) was precipitated out from the reaction mixture. It was collected, washed repeatedly with hot ethanol and dried in vacuum. The other Schiff's bases (**10b–f**) were synthesised accordingly.

Compound 10a: Green solid, yield 92%, IR (KBr) ν_{max}: 2935, 1736, 1605 cm^{-1}; ^{1}H-NMR ($CDCl_3$, 400 MHz): δ_H = 8.38 (s, 1H), 7.77 (d, 2H, J = 8.4 Hz), 7.51 (d, 2H, J = 8.7 Hz), 7.07 (d, 1H, J = 3.9 Hz), 7.02 (d, 1H, J = 3.6 Hz), 6.93 (d, 2H, J = 9.0 Hz), 6.89 (d, 2H, J = 8.7 Hz), 5.36 (d, 1H, J = 4.0 Hz), 4.60–4.63 (m, 1H), 3.96–4.04 (m, 4H), 0.67–2.34 (m, 62H); ^{13}C ($CDCl_3$, 125 MHz): δ_C = 173.0, 161.8, 158.9, 155.2, 153.7, 139.7, 139.3, 130.3, 128.8, 126.8, 124.5, 122.7, 121.3, 114.9, 114.8, 73.8, 68.2, 67.8, 56.7, 56.1, 50.0, 42.3, 39.7, 39.5, 38.2, 37.0, 36.6, 36.2, 35.8, 34.6, 31.9, 31.6, 29.2, 28.9, 28.2, 28.0, 27.8, 25.7, 25.6, 24.8, 24.3, 23.9, 22.8, 22.6, 22.5, 21.0, 19.3, 18.7, 14.0, 11.8; Anal. Calcd. for $C_{56}H_{79}NO_4S$: C, 78.00, H, 9.23, N, 1.62; found: C, 77.87, H, 9.05, N, 1.51%.

Compound 10b: Pale green solid, yield 98%, IR (KBr) ν_{max}: 2925, 1729, 1605 cm^{-1}; ^{1}H-NMR ($CDCl_3$, 400 MHz): δ_H = 8.38 (s, 1H), 7.78 (d, 2H, J = 8.4 Hz), 7.51 (d, 2H, J = 8.8 Hz), 7.07 (d,1H, J = 4.0 Hz), 7.02 (d, 1H, J = 4.0 Hz), 6.94 (d, 2H, J = 8.8 Hz), 6.87 (d, 2H, J = 8.8 Hz), 5.36 (d, 1H, J = 4.0 Hz), 4.57–4.65 (m, 1H), 3.96–4.04 (m, 4H), 0.66–2.31 (m, 72H); ^{13}C ($CDCl_3$, 125 MHz): δ_C = 173.3, 161.8, 158.9, 155.2, 153.7, 139.7, 139.3, 130.2, 128.7, 127.2, 126.8, 124.4, 122.6, 121.3, 114.9, 114.8, 73.7, 68.2, 56.7, 56.2, 50.0, 42.3, 39.8, 39.5, 38.2, 37.0, 36.6, 36.2, 35.8, 34.7, 31.9, 31.6, 29.4, 29.3, 29.2, 29.1, 28.2, 28.0, 27.8, 26.0, 25.7, 25.0, 24.3, 23.8, 22.8, 22.6, 22.59, 21.07, 19.3, 18.7, 14.0, 11.9; Anal. Calcd. for $C_{61}H_{89}NO_4S$: C, 78.57, H, 9.62, N, 1.50; found: C, 78.38, H, 9.45, N, 1.31%.

Compound 10c: Green solid, yield 94%, IR (KBr) ν_{max}: 2931, 1728, 1604 C cm^{-1}; ^{1}H-NMR ($CDCl_3$, 400 MHz): δ_H = 8.38 (s, 1H), 7.78 (d, 2H, J = 8.8 Hz), 7.51 (d, 2H, J = 8.8 Hz), 7.07 (d, 1H, J = 4.0 Hz), 7.02 (d, 1H, J = 3.6 Hz), 6.93 (d, 2H, J = 8.8 Hz), 6.89 (d, 2H, J = 8.4 Hz), 5.36 (d, 1H, J = 4.0 Hz), 4.60–4.62 (m, 1H), 3.96–4.04 (m, 4H), 0.66–2.34 (m, 66H). ^{13}C-NMR ($CDCl_3$, 125 MHz): δ_C = 173.0, 161.6, 158.9, 155.2, 153.6, 139.6, 139.3, 130.2, 128.8, 127.1, 126.8, 124.5, 122.6, 121.3, 114.9, 114.7, 73.8, 68.1, 56.7, 56.1, 50.0, 42.3, 39.5, 36.6, 31.9, 31.8, 29.4, 29.3, 28.2, 28.0, 26.0, 22.8, 22.6, 22.5, 19.3, 18.7, 14.1, 11.9. Anal. Calcd. for $C_{58}H_{83}NO_4S$: C, 78.24, H, 9.40, N, 1.57; found: C, 78.07, H, 9.25, N, 1.40%.

Compound 10d: Green solid, yield 95%, IR (KBr) ν_{max}: 2932, 1733, 1606 cm^{-1}; ^{1}H-NMR ($CDCl_3$, 400 MHz): δ_H = 8.38 (s, 1H), 7.78 (d, 2H, J = 8.8 Hz), 7.51 (d, 2H, J = 8.8 Hz), 7.07 (d, 1H, J = 3.6 Hz), 7.02 (d, 1H, J = 4.0 Hz), 6.94 (d, 2H, J = 8.8 Hz), 6.89 (d, 2H, J = 8.8 Hz), 5.36 (d, 1H, J = 4.0 Hz), 4.60–4.62 (m, 1H), 3.96–4.02 (m, 4H), 0.67–2.31 (m, 76H); ^{13}C ($CDCl_3$, 125 MHz): δ_C = 173.3, 161.8, 158.9, 155.2,

153.7, 139.7, 139.3, 130.3, 128.7, 127.2, 126.8, 124.4, 122.6, 121.3, 114.9, 114.8, 73.7, 68.2, 56.7, 56.2, 50.0, 42.3, 39.8, 39.6, 38.2, 37.0, 36.6, 36.2, 35.8, 34.7, 31.9, 31.8, 29.5, 29.3, 29.2, 29.1, 28.2, 28.0, 27.9, 26.0, 25.0, 24.3, 23.8, 22.8, 22.7, 21.0, 19.3, 18.7, 14.1, 11.9; Anal. Calcd. for $C_{63}H_{93}NO_4S$: C, 78.78, H, 9.76, N, 1.46; found: C, 78.57, H, 9.55, N, 1.31%.

Compound 10e: Pale green solid, yield 98%, IR (KBr) ν_{max}: 2921, 1729, 1604 cm^{-1}; ^{1}H-NMR ($CDCl_3$, 400 MHz): δ_H = 8.38 (s, 1H), 7.78 (d, 2H, J = 8.8 Hz), 7.51 (d, 2H, J = 8.8 Hz), 7.07 (d, 1H, J = 4.0 Hz), 7.02 (d, 1H, J = 4.0 Hz), 6.93 (d, 2H, J = 8.8 Hz), 6.87 (d, 2H, J = 8.8 Hz), 5.36 (d, 1H, J = 4.0 Hz), 4.57–4.65 (m, 1H), 3.94–4.04 (m, 4H), 0.66–2.34 (m, 74H); ^{13}C ($CDCl_3$, 125 MHz): δ_C = 173.0, 161.6, 158.9, 155.2, 153.7, 139.7, 137.3, 130.3, 128.8, 127.2, 126.8, 124.4, 122.6, 121.3, 114.9, 114.8, 73.8, 68.2, 67.8 56.7, 56.2, 50.0, 42.3, 39.8, 39.6, 38.2, 37.0, 36.6, 36.2, 35.8, 34.6, 31.9, 29.7, 29.4, 29.3, 28.2, 27.8, 28.0, 26.0, 25.6, 24.8, 24.9, 23.8, 22.8, 22.7, 22.6, 21.0, 19.3, 18.7, 14.1, 11.9; Anal. Calcd. for $C_{62}H_{91}NO_4S$: C, 78.68, H, 9.69, N, 1.48; found: C, 78.49, H, 9.51, N, 1.29%.

Compound 10f: Green solid, yield 93%, IR (KBr) ν_{max}: 2918, 1736, 1607 cm^{-1}; ^{1}H-NMR ($CDCl_3$, 400 MHz): δ_H = 8.38 (s, 1H), 7.78 (d, 2H, J = 8.8 Hz), 7.51 (d, 2H, J = 8.8 Hz), 7.07 (d, 1H, J = 4.0 Hz), 7.02 (d, 1H, J = 4.0 Hz), 6.94 (d, 2H, J = 8.8 Hz), 6.89 (d, 2H, J = 8.8 Hz), 5.36 (d, 1H, J = 3.6 Hz), 4.60–4.62 (m, 1H), 3.96–4.03 (m, 4H), 0.67–2.31 (m, 84H); ^{13}C ($CDCl_3$, 125 MHz): δ_C = 173.3, 161.8, 158.9, 155.2, 153.7, 139.7, 137.3, 130.2, 128.7, 127.2, 126.8, 124.4, 122.6, 121.3, 114.9, 114.8, 73.7, 68.2, 56.7, 56.2, 50.0, 42.3, 39.8, 39.5, 38.2, 37.0, 35.8, 34.7, 31.9, 29.7, 29.6, 29.5, 29.4, 29.3, 29.2, 29.1, 28.2, 28.0, 26.0, 25.0, 24.3, 23.8, 22.8, 22.7, 22.6, 21.0, 19.3, 18.7, 14.1, 11.9; Anal. Calcd. for $C_{67}H_{101}NO_4S$: C, 79.16, H, 10.01, N, 1.38; found: C, 78.99, H, 9.82, N, 1.19%.

Downloaded by [University of Haifa Library] at 00:18 10 September 2013

Acknowledgements

We thank the DST (New Delhi) and the CSIR (New Delhi) for financial assistance. Two of us (T.G. and S.C.) are grateful to the CSIR (New Delhi) for their research fellowships. We are grateful to Dr C.V. Yelamaggad for molecular modelling of the compound **10c** reported in this publication.

References

[1] Bäuerle, P. In *Oligothiophenes*: Müllen, K., Wegner, G., Eds.; Wiley-VCH: Weinheim, 1998.
[2] Zhang, H.; Shiino, S.; Shishido, A.; Kanazawa, A.; Tsutsumi, O.; Shiono, T.; Ikeda, T. *Adv. Mater. (Weinheim, Ger.)* **2000**, *12*, 1336–1339.
[3] O'Neil, M.; Kelly, S.M. *Adv. Mater. (Weinheim, Ger.)* **2003**, *15*, 1135–1146.
[4] Park, Y.S.; Kim, D.; Lee, H.; Moon, B. *Org. Lett.* **2006**, *8*, 4699–4702.
[5] Geelhaar, T. *Ferroelectrics* **1988**, *85*, 329–349.
[6] Barbarella, G.; Zambianchi, M.; Pudova, O.; Paladini, V.; Ventola, A.; Cipriani, F.; Gigli, G.; Cingolani, R.; Citro, G. *J. Am. Chem. Soc.* **2001**, *123*, 11600–11607.
[7] Lagerwall, S.T. *Ferroelectric and Antiferroelectric Liquid Crystals*; Wiley-VCH: Weinheim, 1999.
[8] Jones, J.C.; Towler, M.J.; Hughes, J.R. *Displays* **1993**, *14*, 86–93.
[9] Wang, H.; Shao, R.; Zhu, C.; Bai, B.; Gong, C.; Zhang, P.; Li, F.; Li, M.; Clark, N.A. *Liq. Cryst.* **2008**, *35*, 967–974.
[10] Imrie, C.T.; Henderson, P.A. *Curr. Opin. Colloid Interface Sci.* **2002**, *7*, 298–311.
[11] Majumdar, K.C.; Chakravorty, S.; Pal, N.; Rao, N.V.S. *Tetrahedron* **2009**, *65*, 152–157.
[12] Majumdar, K.C.; Mondal, S.; Pal, N.; Sinha, R.K. *Tetrahedron Lett.* **2009**, *50*, 1992–1995.
[13] Yelamaggad, C.V.; Mathews, M.; Fujita, T.; Iyi, N. *Liq. Cryst.* **2003**, *30*, 1079–1087.
[14] Yelamaggad, C.V.; Sashikala, I.; Hiremath, U.S.; Rao, D.S.S.; Prasad, S.K. *Liq. Cryst.* **2007**, *34*, 153–167.
[15] Mallia, V.A.; Tamaoki, N. *Chem. Commun.* **2004**, 2538–2539.
[16] Toh, C.L.; Xu, J.; Lu, X.; He, C. *Liq. Cryst.* **2008**, *35*, 241–251.
[17] Bai, B.; Wang, H.; Zhang, P.; Qu, S.; Li, F.; Yu, Z.; Long, B.; Li, M. *Liq. Cryst.* **2008**, *35*, 793–798.
[18] Wang, H.; Shao, R.; Zhu, C.; Bai, B.; Gong, C.; Zhang, P.; Li, F.; Li, M.; Clark, N.A. *Liq. Cryst*. **2008**, *35*, 967–974.
[19] Centore, R. *Liq. Cryst.* **2009**, *36*, 239–245.
[20] Bialecka-Florjanczyk, E.; Sledzinska, I.; Gorecka, E.; Przedmojski, J. *Liq. Cryst.* **2008**, *35*, 401–406.
[21] Bhowmik, P.K.; Han, H.; Nedeltchev, A.K.; Mandal, H.D.; Jimenez-Hernandez, J.A.; McGannon, P.M.; Lopez, L.; Kang, S.W.; Kumar, S. *Liq. Cryst.* **2009**, *36*, 1389–1399.
[22] Ferrarini, A.; Greco, C.; Luckhurst, G.R. *J. Mater. Chem*. **2007**, *17*, 1039–1042.
[23] Aziz, N.; Kelly, S.M.; Duffy, W.; Goulding, M. *Liq. Cryst*. **2008**, *35*, 1279–1292.
[24] Srivastava, R.M.; Filho, R.A.W.N.; Schneider, R.; Vieira, A.A.; Gallardo, H. *Liq. Cryst*. **2008**, *35*, 737–742.
[25] Attard, G.S.; Date, R.W.; Imrie, C.T.; Luckhurst, G.R.; Roskilly, S.J.; Seddon, J.M.; Taylor, L. *Liq. Cryst.* **1994**, *16*, 529–581.
[26] Imrie, C.T. *Liq. Cryst.* **2006**, *33*, 1449–1454.
[27] Attard, G.S.; Garnett, S.; Hickman, C.G.; Imrie, C.T.; Taylor, L. *Liq. Cryst.* **1990**, *7*, 495–508.
[28] Kitzerow, H.-S., Bahr, C., Eds. *Chirality in Liquid Crystal*; Springer-Verlag: New York, 2001.
[29] Kitzerow, H.-S. *Chem. Phys. Chem.* **2006**, *7*, 63–66.
[30] Goodby, J.W. In *Handbook of Liquid Crystal*: Demus, D., Goodby, J.W., Gray, G.W., Spiess, H.-W., Eds.; Wiley-VCH: Weinheim, New York, 1998; Vol.1, Ch. V, p 115.
[31] Yelamaggad, C.V.; Achalkumar, A.S.; Bonde, N.L.; Prajapati, A.K. *Chem. Mater.* **2006**, *18*, 1076–1078.
[32] Yelamaggad, C.V.; Bonde, N.L.; Achalkumar, A.S.; Rao, D.S.S.; Prasad, S.K.; Prajapati, A.K. *Chem. Mater.* **2007**, *19*, 2463–2472.

[33] Majumdar, K.C.; Mondal, S.; Sinha, R.K. *New J. Chem*. **2010**, *34*, 1255–1260.
[34] Mallia, V.A.; Tamaoki, N. *Chem. Mater.* **2003**, *15*, 3237–3239.
[35] Yelamaggad, C.V.; Shanker, G.; Hiremath, U.S.; Prasad, S.K. *J. Mater. Chem.* **2008**, *18*, 2927–2949.
[36] Zhang, C.; Jin, L.; Yin, B.; Jamil, M.; Jeon, Y.J. *Liq. Cryst*. **2008**, *35*, 39–44.
[37] Sharma, R.K.; Gupta, V.K.; Mathews, M.; Yelamaggad, C.V. *Liq. Cryst*. **2008**, *35*, 1161–1167.
[38] Pandey, A.S.; Dhar, R.; Pandey, M.B.; Achalkumar, A.S.; Yelamaggad, C.V. *Liq. Cryst*. **2009**, *36*, 13–19.
[39] Sharma, R.K.; Gupta, V.K.; Mathews, M.; Yelamaggad, C.V. *Liq. Cryst.* **2009**, *36*, 225–230.
[40] Imrie, C.T.; Henderson, P.A. *Chem. Soc. Rev.* **2007**, *36*, 2096–2124.
[41] Imrie, C.T.; Henderson, P.A.; Yeap, G.Y. *Liq. Cryst.* **2009**, *36*, 755–777.
[42] Dierking, I.; Gie*β*elmann, F.; Zugenmaier, P.; Kuczynski, W.; Lagerwall, S.T.; Stebler, B. *Liq. Cryst.* **1993**, *13*, 45–55.
[43] Dierking, I. *Liq. Cryst.* **1999**, *26*, 83–95.
[44] Donaldson, T.; Staesche, H.; Lu, Z.B.; Henderson, P.A.; Achard, M.F.; Imrie, C.T. *Liq. Cryst.* **2010**, *37*, 1097–1110.
[45] Blatch, A.E.; Fletcher, I.D.; Luckhurst, G.R. *J. Mater. Chem.* **1997**, *7*, 9–17.
[46] Yeap, G.Y.; Hng, T.C.; Yeap, S.Y.; Gorecka, E.; Ito, M.M.; Ueno, K.; Okamoto, M.; Mahmood, W.A.K.; Imrie, C.T. *Liq. Cryst*. **2009**, *36*, 1431–1441.
[47] Imrie, C.T. *Liq. Cryst.* **1989**, *6*, 391–396.
[48] Attard, G.S.; Imrie, C.T.; Karasz, F.E. *Chem. Mater*. **1992**, *4*, 1246–1253.
[49] Attard, G.S.; Imrie, C.T. *Liq. Cryst*. **1992**, *11*, 785–789.
[50] Sandhya, K.L.; Prasad S.K.; Rao, D.S.S.; Bahr, C. *Phys. Rev. E: Stat., Nonlinear, Soft Matter Phys.* **2002**, *66*, 031710.
[51] Aldred, M.P.; Hudson, R.; Kitney, S.R.; Vlachos, P.; Liedtke, A.; Woon, K.L.; O'Neill, M.; Kelly, S.M. *Liq. Cryst.* **2008**, *35*, 413–427.
[52] Yeap, G.-Y.; Hung, T.-C.; Takeuchi, D.; Osakada, K.; Mahmood, W.A.K.; Ito, M.M. *Mol. Cryst. Liq. Cryst.* **2009**, *506*, 134–149.
[53] Seed, A.J.; Cross, G.J.; Toyne, K.J.; Goodby, J.W. *Liq. Cryst.* **2003**, *30*, 1089–1107.

Downloaded by [University of Haifa Library] at 00:18 10 September 2013